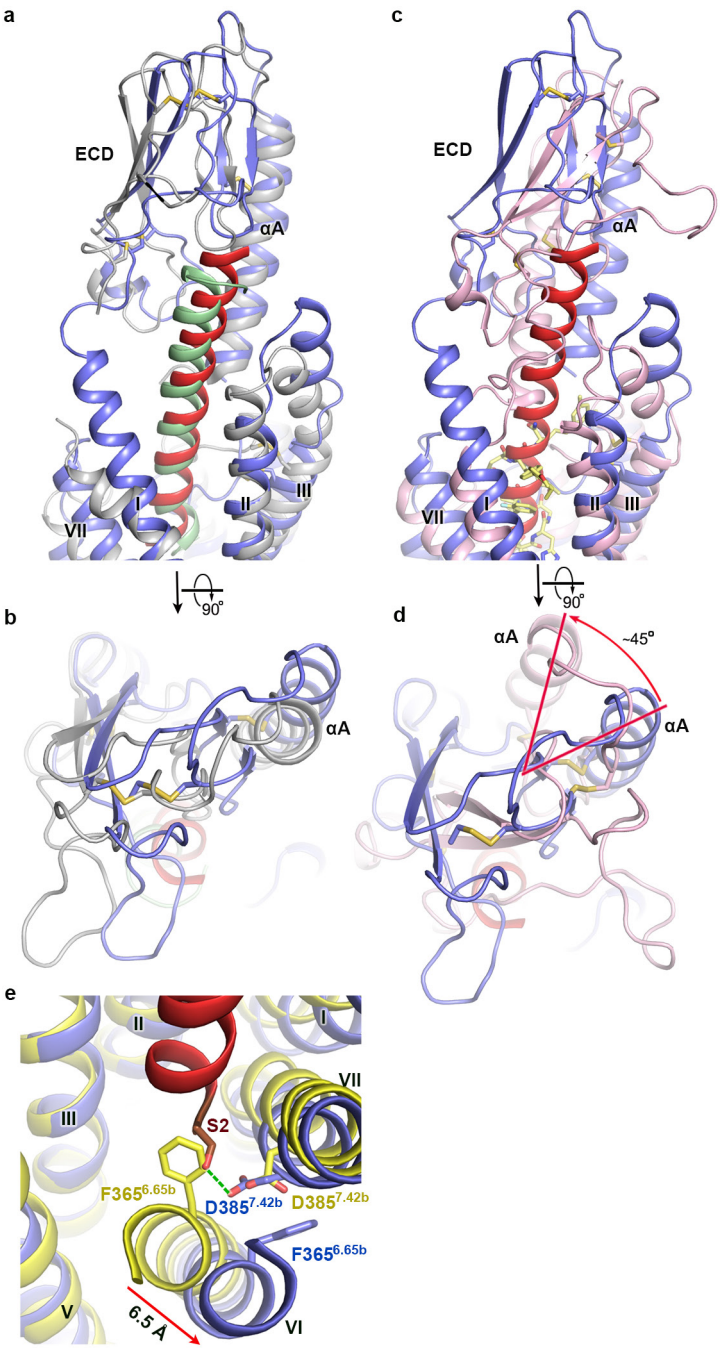

Extended Data Figure 2 | Structural comparison between the GCGR–NNC1702 crystal structure and previously solved class B GPCR structures. a, **b**, Comparison between the GCGR–NNC1702 crystal structure and the cryo-electron microscopy structure of GLP-1–GLP-1R–Gs complex in side (**a**) and extracellular (**b**) views. The GCGR–NNC1702 structure is shown in cartoon representation and coloured blue (GCGR) and red (NNC1702). The GLP-1–GLP-1R–Gs electron microscopy structure (PDB ID: 5VAI) is shown in cartoon representation and coloured grey (GLP-1R) and green (GLP-1). **c**, **d**, Comparison between the crystal structures of the GCGR–NNC1702 and GLP-1R–peptide 5 complexes in side (**c**) and extracellular (**d**) views. The receptor in the GLP-1R–peptide 5 structure (PDB ID: 5NX2) is shown in cartoon representation and coloured pink. The ligand peptide 5 is shown as yellow sticks. The red arrow (in **d**) indicates the rotation of the ECD in the GLP-1R–peptide 5 structure compared to the GCGR–NNC1702 structure. **e**, Comparison between the GCGR–NNC1702 structure and the GCGR–NNC0640–mAb1 structure. Only the GCGR TMD in both structures and the peptide ligand NNC1702 are shown as cartoons. The TMD in the GCGR–NNC1702 structure is in blue; the TMD in the NNC0640-bound structure is in yellow; and NNC1702 is in red. A close inspection of the two full-length GCGR structures revealed a spatial hindrance caused by the residue S2 of NNC1702 and its contact with $D385^{7.42b}$ in the peptide-bound structure, pushing the residue $F365^{6.56b}$ on helix VI away from the ligand-binding pocket and subsequently leading to the outward shift of the extracellular portion of helix VI (red arrow). The residues $F365^{6.65b}$ and $D385^{7.42b}$ in both structures are displayed as sticks. The hydrogen bond between S2 and $D385^{7.42b}$ in the peptide-bound structure is shown as a green dashed line.